American Journal of Pathology, Vol. 166, No. 1, January 2005

Molecular Pathogenesis of Genetic and Inherited Diseases

Brain and Bone Damage in KARAP/DAP12 Loss-of-Function Mice Correlate with Alterations in Microglia and Osteoclast Lineages

Serge Nataf,* Adrienne Anginot,† Carine Vuaillat,* Luc Malaval,‡ Nassima Fodil,§ Emmanuel Chereul,¶ Jean-Baptiste Langlois,¶ Christiane Dumontel,* Gaelle Cavillon,* Christian Confavreux,* Marlène Mazzorana,† Laurence Vico,‡ Marie-Franaçoise Belin,* Eric Vivier,§ Elena Tomasello,§ and Pierre Jurdic†

From INSERM U433, Faculté Laennec, Lyon; UMR 5161 CNRS/ENS, Unité Mixte de la Recherche Institut National de la Recherche Agronomique/Centre National de la Recherche Scientifique 1237,† Ecole Normale Supérieure, Lyon; Plate-forme ANIMAGE (Rhône-Alpes Genopole), Bat. Cermep, Lyon; Centre d'Immunologie de Marseille-Luminy,§ CNRS-INSERM, Université de la Méditerranée, Marseille; and Laboratoire de Biologie du Tissue Osseux INSERM E0366,‡ Faculté de Médecine, Université Jean Monnet, Saint-Etienne, France*

Human polycystic lipomembraneous osteodysplasia with sclerosing leukoencephalopathy, also known as Nasu-Hakola disease, has been described to be associated with mutations affecting the immunoreceptor tyrosine-based activation motif-bearing KARAP/DAP12 immunoreceptor gene. Patients present bone fragilities and severe neurological alterations leading to presenile dementia. Here we investigated whether the absence of KARAP/DAP12-mediated signals in loss-of-function (KΔ75) mice also leads to bone and central nervous system pathological features. Histological analysis of adult KΔ75 mice brains revealed a diffuse hypomyelination predominating in anterior brain regions. As this was not accompanied by oligodendrocyte degeneration or microglial cell activation it suggests a developmental defect of myelin formation. Interestingly, in postnatal KΔ75 mice, we observed a dramatic reduction in microglial cell numbers similar to *in vitro* microglial cell differentiation impairment. Our results raise the intriguing possibility that defective microglial cell differentiation might be responsible for abnormal myelin development. Histomorphometry revealed that bone remodeling is also altered, because of a resorption defect, associated with a severe block of *in vitro* osteoclast differentiation. In addition, we show that, among monocytic lineages, KARAP/DAP12 specifically controls microglial and osteoclast differentiation. Our results confirm that KARAP/DAP12-mediated signals play an important role in the regulation of both brain and bone homeostasis. Yet, important differences exist between the symptoms observed in Nasu-Hakola patients and KΔ75 mice. *(Am J Pathol 2005, 166:275–286)*

KARAP (also called DAP12 or TYROBP), as well as the closely related adaptors CD3ζ and FcRγ, belongs to the family of ITAM (immunoreceptor tyrosine-based activation motif)-bearing signaling adaptors.[1,2] It was first described to be associated with the activating isoforms of NK receptors specific for MHC class I, as well as with the NCR (natural cytotoxicity receptor) NKp44 in humans and with the NKG2D-S receptor in mice.[3–5] Its expression is not restricted to NK cells, but characterizes also several myeloid lineages. Myeloid KARAP/DAP12-associated activating receptors include human SIRP-β1 and MDL-1.[6–8] In addition, KARAP/DAP12 is associated with several members of the TREM (triggering receptor expressed on myeloid cells) family, including TREM-2, which is expressed on monocyte-derived dendritic cells (DCs) as well as in osteoclasts and microglia.[9]

A pathology related to KARAP/DAP12 or TREM2 deficiencies has been described in humans. Human PLOSL (polycystic lipomembraneous osteodysplasia with scle-

Supported by INSERM Centre National de la Recherche Scientifique (grant "Groupe Inter Scientifique maladies rares" 2003 to S.N., E.N., and P.J.), the Ligue Nationale Contre le Cancer ("Equipe labelisée" to E.V., N.F., and E.T.), the Fondation pour la Recherche Médicale (postdoctoral fellowship to S.N.), the Rhône-Alpes region (to S.N.), the Lyons Club–Village Beaujolais (to G.C.), the French Ministry of Research (to A.A.), and the Association pour la Recherche Contre le Cancer (to N.F.).

S.N. and A.A. contributed equally to this work.

Accepted for publication October 5, 2004.

Address reprint requests to P. Jurdic, Ecole Normale Supérieure, 46 Allée d'Italie, 69364 Lyon Cedex 07, France. E-mail: pjurdic@ens-lyon.fr.

rosing leukoencephalopathy), also known as Nasu-Hakola disease, is an inherited genetic disorder affecting predominantly Finnish and Japanese individuals. Mutation of the KARAP/DAP12 gene corresponds to a deletion encompassing exons 1 to 4 in the Finnish cohort, whereas a single-base deletion leading to a stop mutation is present in exon 3 of the Japanese cohort.[10] These patients suffer from spontaneous fractures because of bone cysts and develop presenile dementia leading to premature death at 40 to 50 years of age.[10,11] The existence has also been reported of some PLOSL patients without defects in the KARAP/DAP12 gene, but with distinct mutations in the gene encoding for the human KARAP/DAP12-associated receptor TREM-2.[12–14] Humphrey and colleagues[15] recently confirmed that TREM-2 pairs with KARAP/DAP12 in the osteoclast lineage. Interestingly, it was recently described that KARAP/DAP12 knockout mice present a developmental arrest of oligodendrocytes as well as hypomyelination in the thalamus[16] and, in contrast to human pathology, a mild osteopetrosis because of osteoclasts being unable to resorb bone.[16–19]

In the developing brain, neurons, astrocytes, and the central nervous system (CNS) myelin-forming cells, oligodendrocytes, arise from a common neuroepithelial precursor. Myelin formation is a long-lasting process that is fully completed a long time after birth. It requires a number of signals that are intrinsic to oligodendrocytes or delivered by their microenvironment, particularly axons[20] and astrocytes.[21] In contrast with these cell types, it is currently admitted that microglia are ontogenetically related to the immune system and derived from hematopoietic stem cells,[22] more precisely myeloid progenitors.[23] Indeed, microglia in their activated form, amoeboid microglia, invade the developing CNS, where they mainly permit the phagocytosis of cellular debris. However, the full range of functions that microglia may play during CNS development remains primarily unknown.

Bone remodeling is a physiological process tuned by the balance between the synthesis of bone matrix, controlled by osteoblasts of mesenchymal origin, and bone resorption, regulated by osteoclasts that derive from hematopoietic precursors of the monocytic lineage.[24] *In vitro* differentiation of osteoclasts from the hematopoietic tissues of KARAP/DAP12-deficient mice in the presence of M-CSF and RANKL is completely impaired[16–19] whereas osteoclasts are present *in vivo*. This observation has allowed a new pathway to be deciphered, in addition to RANKL-RANK, involved in late osteoclast differentiation. Still unknown ligands, provided by osteoblasts or other cell types, bind to receptors including TREM-2 and OSCAR to transduce activating signals via FcRγ and KARAP/DAP12 adaptors and syk tyrosine kinase activation.[17,18]

In the present study, we have used mice harboring a mutated KARAP/DAP12 loss-of-function molecule (KΔ75) in the ITAM domain.[25] A deletion of the second part of the ITAM domain, including the C terminal tyrosine (Y75), has been made, this resulting in the KΔ75 protein, expressed but not functional, being unable to phosphorylate its downstream targets. We have investigated whether pathological alterations observed in bone and brain of Nasu-Hakola patients, as well as in KARAP/DAP12 knockout mice, were recapitulated in KΔ75 mice, then dependent only of the ITAM domain activity. Moreover, because osteoclasts and microglial cells share a myeloid origin and we have previously identified a common bone marrow precursor for these two cell types, as well as for macrophages and DCs,[23] we studied the role of the KARAP/DAP12 ITAM domain in the commitment of monocytic precursors.

Materials and Methods

Mice

KΔ75 loss-of-function mice used in all of the experiments derive from eight backcrosses with C57BL/6 mice.[25] Age- and sex-matched wild-type (WT) C57BL/6 mice (CDTA, Orleans, France) were used as controls, unless indicated. Mice were kept and bred under specific pathogen-free conditions, and sacrificed by CO_2 inhalation.

In Vitro *Amplification and Differentiation of Murine Monocytic Cells*

Bone marrow from 6- to 8-week mice long bones was flushed and cultured in the presence of Flt3L as described.[23] Cells were then differentiated into macrophages, osteoclasts, DCs, or microglia cells in the presence of the appropriate cytokines or glial cell-conditioned medium for microglia.[23] Macrophages and DC maturation were evaluated by fluorescence-activated cell sorting (FACS) analysis for specific surface marker expression using an anti-mouse F4/80 antibody (Sigma, St. Louis, MO), or anti-mouse MHC class II and anti-mouse CD40 antibodies (Pharmingen, San Diego, CA), respectively. A functional analysis of macrophages was performed to test their capacity to phagocyte latex beads (Sigma, St. Louis, MO). Osteoclast differentiation was evaluated by the presence of tartrate-resistant acid phosphatase (TRAP)-positive multinucleated cells, comprising more than three nuclei, using the leukocyte acid phosphatase kit (Sigma). Microglial cell differentiation was assessed following morphological criteria previously described.[23,26]

In Vitro *Differentiation of Murine Osteoclasts*

Total bone marrow from 6- to 8-week-old mice was extracted by perfusion of the tibia and fibula with α-minimum essential medium (Life Technologies, France) supplemented with 200 μg/ml penicillin/streptomycin, 2 mmol/L glutamine (Invitrogen, France), and 10% fetal bovine serum (Hyclone, Perbio, Bezans, France). Cells were plated at 10^4 cells/mm^2 in this medium supplemented with recombinant murine monocyte-colony stimulating factor (M-CSF) and recombinant RANKL, or 10 nmol/L 1α,25(OH_2) vitamin D3 (Leo Pharmaceutical Products, Denmark) or 100 nmol/L fragment 1-34 PTH (parathyroid hormone, Sigma). Resorption tests were per-

formed on dentin slices and toluidine blue was used to reveal resorption pits after cell removal.[27]

Reverse Transcriptase-Polymerase Chain Reaction Analysis

mRNA were extracted with RNAnow reagent (Biogentex, Seabrook, TX) from bone marrow cell cultures (*in vitro* samples) or directly from bones crushed in liquid nitrogen (*in vivo* samples). Aliquots (1 μg) were reverse-transcribed using the MuLV-RT kit (Promega, Madison, WI). Polymerase chain reaction was performed with specific primers using the *Taq* polymerase kit (Eurobio, Les Ulis, France). Primers used were calcitonin receptor (CTR) 5′: TGGTTGAGGTTGTGCCCAATGGAGA; CTR 3′: CTCGTGG GTTTG CCTCATCTTGGTC; cathepsin K 5′: TTAATTTGGGAGAAAAACCT; cathepsin K 3′: AGCCGCCTCCACAGCCATAAT; GAPDH 5′: CAAAGTGGAGATTGTTGCCAT; GAPDH 3′: CACCACCTTCTTGATGTCATC. Amplifications were done for 24 cycles for GAPDH and 34 cycles for CTR and cathepsin K.

Electron Microscopy

For electron microscopy analysis, brains from two KΔ75 and two control mice aged between 8 and 10 months were fixed with 4% paraformaldehyde and 2% glutaraldehyde. A first neuropathological examination of brains was performed by toluidine blue staining on 1-μm sections of anterior brain regions embedded in Epon. Further analysis was performed on ultrathin transverse sections of the striatum, corpus callosum, and frontal cortex. In addition, in two KΔ75 mice and two control mice, a quantitative analysis of axonal diameters and myelin sheath thickness was performed on transverse sections of white matter tracts crossing the striatum. For this purpose, 10 randomly chosen fields were examined at $\times$20,000 magnification and measures of axonal diameters ($n = 254$ and $n = 245$ for KΔ75 and control mice, respectively) and myelin sheath thicknesses ($n = 330$ and $n = 315$ for KΔ75 and control mice, respectively) were recorded using image analysis software (Analysis 3.2, Soft Imaging System).

Immunohistofluorescence

Brains isolated from KΔ75 or control mice between 8 and 10 months of age, were surgically removed, snap-frozen in liquid nitrogen-chilled isopentane and stored at −80°C. Immunohistofluorescence analysis was performed on 14-μm-thick horizontal brain sections as follows. Sections were fixed in ethanol at room temperature for 10 minutes and then incubated in a blocking solution containing 4% bovine serum albumin and 10% normal goat serum. Sections were then incubated in blocking solution containing one of the following monoclonal antibodies: mouse anti-bovine myelin basic protein (MBP; Serotec, Kidlington, UK), mouse anti-human CNPase (Sigma), rat anti-mouse CD11b; rat anti-mouse MHC class II (BD PharMingen, San Diego, CA), and polyclonal antibodies: mouse anti-human neurofilament (NF) (DAKO, Glostrup, Denmark), mouse anti-neuronal nuclei (NeuN; Chemikon, Temecula, CA); mouse anti-nestin antibody (BD PharMingen). After several washes in phosphate-buffered saline (PBS), sections were incubated for 50 minutes with species-specific fluorescein-conjugated goat secondary antibodies (Interchim, Montluçon, France). Sections were then rinsed in PBS and mounted using Fluoroprep (BioMérieux, Marcy l'Etoile, France).

Ex Vivo *FACS Analysis of Microglial Cells*

Brains obtained from P13 KΔ75 ($n = 6$) or WT mice ($n = 6$) were dissected, homogenized in ice-cold PBS/2% fetal calf serum, and centrifuged at 1600 rpm for 5 minutes at 4°C. In some experiments, brains were pooled into pairs after homogenization. The pellet was resuspended in 4 ml of 70% Percoll and overlaid with 4 ml of 37% Percoll and 4 ml of 30% Percoll as previously described.[28] Percoll gradients were centrifuged at 1600 rpm for 20 minutes at 20°C without a brake, then cells were collected from the 37%/70% Percoll interface, washed once in PBS 1×, counted, and resuspended in PBS/2% fetal calf serum. For immunolabeling, cells were incubated for 30 minutes at 4°C with CD16/CD32 monoclonal antibody (BD Pharmingen, San Diego, CA) then washed in PBS/2% fetal calf serum and incubated for 30 minutes at 4°C with phycoerythrin-labeled anti-CD11b mAb (BD Pharmingen). Cells were then washed in PBS 1× and fixed in 4% paraformaldehyde before being analyzed on a Coulter Epics XL flow cytometer (Beckman Coulter Inc., Fullerton, CA). The total number of $CD11b^+$ cells per brain was calculated as previously described[28] based on 1) the percentage of $CD11b^+$ cells within living cell gated, 2) the number of living cells used for CD11b staining, and 3) the total number of living cells obtained from the Percoll density gradient.

Bone Radiography, Densitometry, and Three-Dimensional Microcomputer Tomography (μCT) Analysis

For X-ray analysis, WT and KΔ75 5-month-old mice were sacrificed by CO_2 inhalation and fixed in 4% paraformaldehyde in PBS for 5 hours at 4°C. Radiographies were made using a cabinet X-ray system (model MX-20; Faxitron X-ray Corp., Wheeling, IL). Exposures were for 35 seconds with an 18 kV X-ray source using Min-R 2000 films (Eastman-Kodak, Rochester, NY). A dual energy X-ray (DEXA) PIXImus densitometer (Lunar Corp., Madison, WI) with small animal software was used to measure bone mineral density and bone mineral content of femurs of the sacrificed mice. Three-dimensional imaging was performed using an *in vivo* X-ray microtomograph (SkyScan 1076; SkyScan, Aartselaar, Belgium). The acquisition parameters were spatial resolution 35 μm, X-ray beam qualities 100kV/100μA with 0.5 mm aluminum fil-

tration, 360° rotation. Three-dimensional reconstruction and quantification were done using SkyScan software.

Bone Histomorphometry

For histological analysis, mice were injected, 5 and 2 days before sacrifice, with 15 mg/kg calcein. The femurs were dissected out, fixed in 4% paraformaldehyde, dehydrated in acetone, and embedded in methylmethacrylate. Longitudinal frontal slices were cut from the embedded bones with a Jung model K microtome (Carl Zeiss, Heidelberg, Germany). Six nonserial sections, 8 μm thick, were used for modified Goldner staining. Fourteen-μm-thick sections were used to determine the dynamic indices of bone formation: percentage of bone trabecular surface labeled with calcein (MS/BS), mineral apposition rate, and bone formation rate/bone surface (BFR/BS).[29] Mineral apposition rate was derived from fluorochrome interlabel distances. BFR was subsequently obtained from the product of MS/BS and mineral apposition rate. Six-μm-thick sections were used for TRAP staining to determine osteoclastic parameters. Bone volume and parameters reflecting trabecular structure were measured using an automatic image analysis system (Biocom, Lyon, France). Bone cellular and macroscopic parameters were measured with a semiautomatic system: a digitizing tablet (Summasketch, Summagraphics, Paris, France) connected to a Macintosh personal computer with software designed in the laboratory. Statistical differences between groups were assessed using Student's *t*-test.

Measurement of Urinary Levels of Deoxypyridinoline (U-DPD)

One hundred fifty μl of urine were collected immediately from each of the mice tested. Amounts of U-DPD were quantified by Synarc Corp. (Lyon, France) using the Metra DPD kit, standardized with creatinine using the Metra creatinine kit (Quidel Corp., Paris, France).

Results

Broadly Distributed Hypomyelination and Absence of Inflammatory Reaction in the Brain of KΔ75 Mice

Neuroimaging and neuropathological analysis performed on brains of human PLOSL patients have revealed frontally accentuated loss of myelin, accompanied by enlarged ventricules, and atrophy of several brain regions. These alterations are most likely related to PLOSL neurological symptoms leading to dementia.[10,11] During CNS development, the great majority of neurons have their axons enwrapped by a myelin sheath composed of specific glycolipids and proteins such as MBP. Myelination requires that oligodendrocytes migrate toward axons and extend cellular processes that spiral around them. To evaluate the level of myelination in KΔ75 as compared to controls, immunofluorescence experiments were performed using anti-MBP or anti-CNPase antibodies on horizontal brain sections. In contrast to control mice (Figure 1; A to C), an abnormal heterogeneous pattern of MBP or CNPase staining was observed in myelin-rich areas of KΔ75 mice anterior brain (Figure 1; E to G). Interestingly, such staining patterns readily detectable in several anterior brain regions (fornix, corpus callosum, white matter tracts of the striatum) can also be observed to a lesser extent in the fimbria hippocampi and cerebellar white matter (data not shown). Thus our results reveal a broadly distributed myelin defect that is localized predominantly to frontal brain regions.

Neuronal cell loss and axonal fragmentation characterized by the presence of neurofilament-positive spheroid bodies has been observed in the brain of PLOSL patients.[10] However, neurofilament staining of brain sections obtained from KΔ75 mice did not display spheroid bodies or obvious axonal alteration of the cytoskeleton (data not shown). In the same way, using an anti-NeuN antibody, neuronal cell density appeared similar in both KΔ75 and control mice when brain cortex, hippocampus, cerebellum, or thalamus were examined (data not shown). Microglial activation and astrocytosis are the main inflammatory features reported in neuropathological examinations of PLOSL patients. However in KΔ75 mice, $CD11b^+$ microglial cells showed a ramified quiescent morphology (Figure 1H) similar to control mice (Figure 1D) and no astrocytosis was observed in all gray and white matter regions examined, a finding confirmed using electron microscopy (data not shown). Brain microvascular changes and microinfarcts possibly leading to the calcification of basal ganglia were reported to occur in PLOSL patients.[10] In KΔ75 mice, the ultrastructure of brain microvessels was normal (data not shown) and at the light microscopy level, calcification was not detected in every area studied, including basal ganglia. Taken together, these data suggest that, in mice, the absence of functional KARAP/DAP12 is associated with an impaired myelinogenesis that, in contrast with PLOSL patients, is not accompanied by inflammation, microvascular changes, or major axonal alterations.

Isolated Reduction of Myelin Sheath with Lack of Oligodendrocyte Degeneration in the Brain of KΔ75 Mice

The heterogeneous MBP or CNPase staining pattern observed in anterior brain regions of KΔ75 mice prompted us to better characterize the myelin and oligodendrocyte status at the ultrastructural level. As the age of onset of nervous alterations in PLOSL patients ranges from 30 to 40 years, we examined brains isolated from 8- to 10-month-old mice. In transversal semithin sections of anterior brain obtained from KΔ75 mice, toluidine blue staining permitted hypomyelination to be detected in the corpus callosum and white matter tracts of the striatum as compared to controls (data not shown). When ultrathin sections of these regions were analyzed by EM, it appeared that numerous axons were either poorly or not at

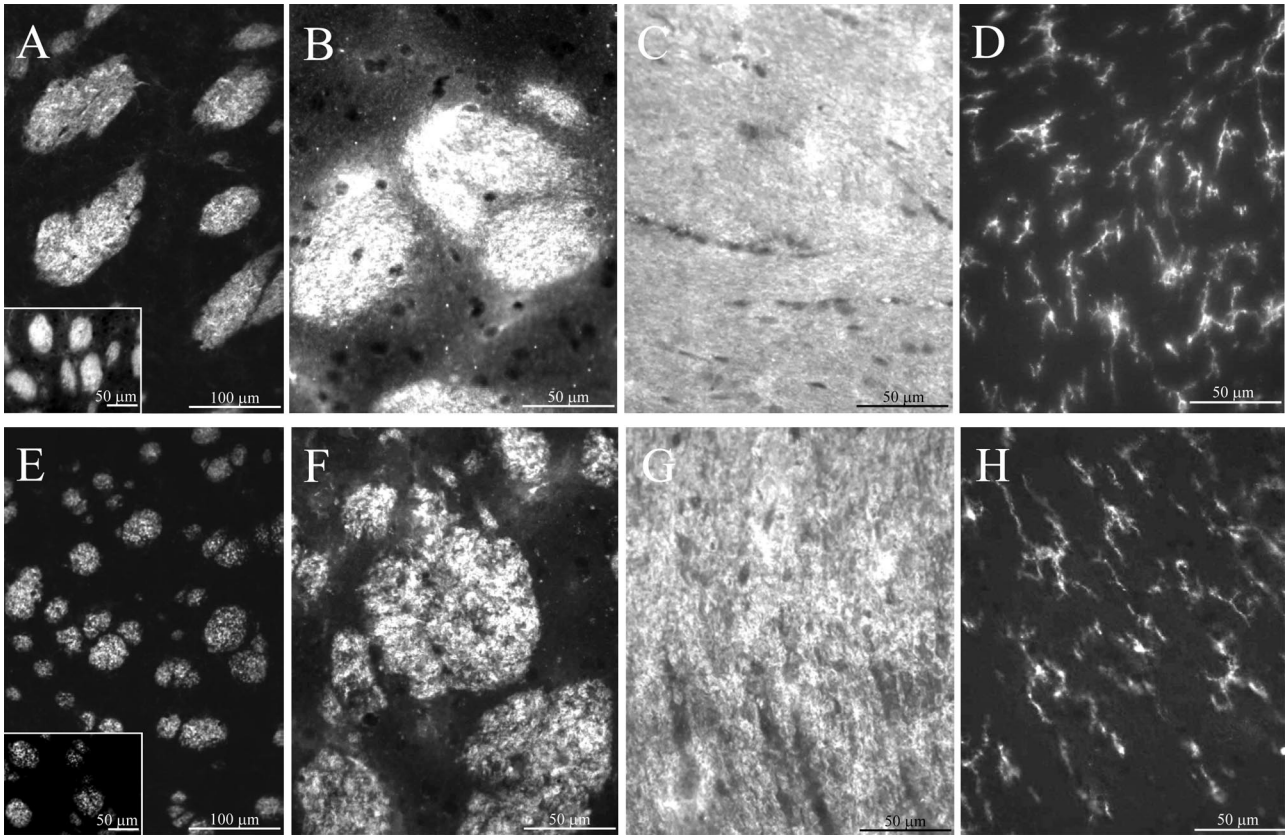

Figure 1. Brain hypomyelination and lack of inflammation in KΔ75 loss-of-function mice. CNPase (**A**, **E**) or MBP staining (**B**, **C**, **F**, **G**) was performed on horizontal brain sections of striatum (**A**, **B**, **E**, **F**) and corpus callosum (**C**, **G**) obtained from control (**A–C**) or KΔ75 mice (**E–G**). **Insets** in **A** and **E** show high-magnification views of CNPase stainings. Note the heterogeneous MBP or CNPase staining pattern observed in KΔ75 mice as compared to controls. CD11b staining was performed on horizontal brain sections of corpus callosum (**D**, **H**). $CD11b^+$ microglial cells have similar morphology when comparing WT (**D**) and KARAP/DAP12 loss-of function mice (**H**). Data are representative of three experiments performed on the 16 mice analyzed.

all myelinated in KΔ75 mice (Figure 2A, right, asterisks) as opposed to controls (Figure 2A, left). At the same time, oligodendrocytes could be detected at an apparently normal density in KΔ75 mice and did not show signs of apoptosis or necrosis (data not shown). Interestingly, the cytoplasmic ultrastructure of unmyelinated axons had an overall normal appearance suggesting that defective myelination does not result from a primarily axonal pathology. Finally, we did not notice any pathological changes in blood vessel structure (data not shown) in contrast with the reported vessel wall thickening observed in brains of Nasu-Hakola patients.[11] To quantify the level of hypomyelination observed in KΔ75 mice, axon diameter and myelin thickness were measured in KΔ75 mice ($n = 2$) and controls ($n = 2$). Myelin thickness measurements confirmed a dramatic hypomyelination in KΔ75 mice (87 ± 18 nm, $n = 330$) as compared to controls (112 ± 17 nm, $n = 315$) (Figure 2B, right). Also, we observed that axon diameters were significantly increased in KΔ75 mice (696 ± 34 nm, $n = 245$) as compared to controls (577 ± 21 nm, $n = 254$) (Figure 2B, left). Although no obvious qualitative alterations were observed in KΔ75 mice regarding axonal ultrastructure, the increased axonal diameter observed in these mice may reflect a certain level of axonal swelling that might occur during secondary axonal pathologies.

Defective Microglial Cell Development in the Brain of Postnatal KΔ75 Mice

Because KARAP/DAP12 was first described as a major activation signal in myeloid cells, we examined the microglial status in KΔ75 or WT mice during the postnatal period. Indeed, this time-frame is characterized by a massive invasion of CNS parenchyma by activated microglia.[30,31] Using immunohistofluorescence as well as *ex vivo* FACS analysis, we observed that P10 or P15 KΔ75 mice show a dramatic decrease in microglial cell numbers as compared to age-matched WT mice (Figure 3, A and C, and Figure 4). However, macrophages associated with meninges were still detectable in P10 or P15 KΔ75 mice (Figure 3C, arrow). In contrast with microglia, astrocyte numbers and morphology did not appear to be altered, as assessed by glial fibrillary acidic protein (GFAP) staining (Figure 3, B and D). The neural stem cell marker, nestin, was recently detected on microglia in primary microglial cell cultures[32] and in an *in vivo* model of posttraumatic gliosis.[33] We therefore analyzed nestin expression by microglia in anterior brain regions of P15 KΔ75 or control mice during postnatal development. As shown in Figure 3E, we observed that in P15 WT mice, a population of ramified $nestin^+$ cells could be detected in

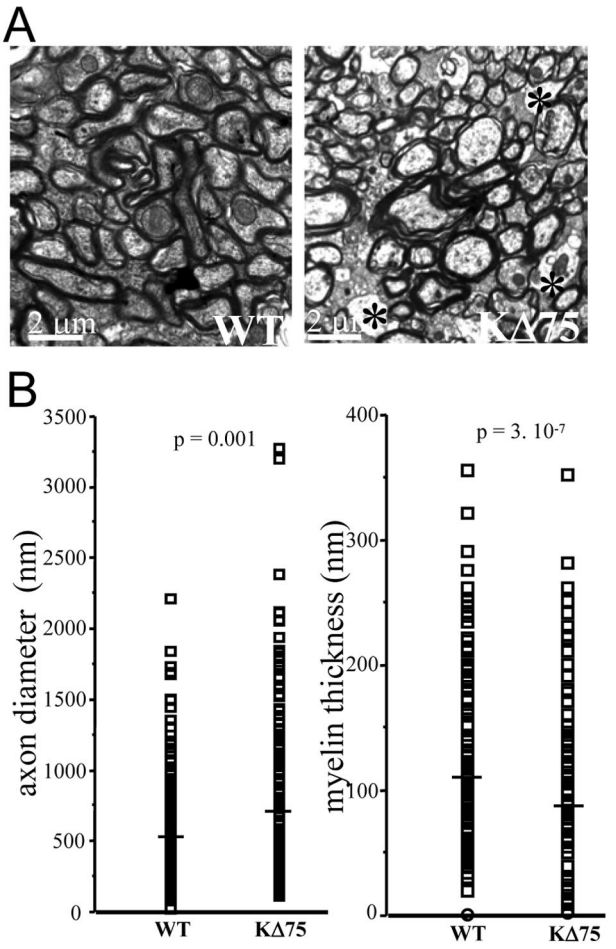

Figure 2. Brain ultrastructural pathology in KΔ75 loss-of-function mice. **A:** Transverse sections of brain striatum isolated from control mice (**left**) or KΔ75 mice (**right**) were analyzed by electron microscopy. Unmyelinated axons in the white matter tracts of a KΔ75 mouse are indicated by **black asterisks**. **B:** Measurements of axon diameter and myelin thickness were performed on KΔ75 mice (n = 2) and controls (n = 2). Mean myelin thickness is dramatically decreased in KΔ75 mice (87 ± 18 nm, n = 330) as compared to controls (112 ± 17 nm, n = 315, $P = 3.10^{-7}$ with unequal variance, Student's t-test) (**right**). In contrast, mean axon diameter is significantly increased in KΔ75 mice (696 ± 34 nm, n = 245) as compared to controls (577 ± 21 nm, n = 254, P = 0.001 with unequal variance, Student's t-test) (**left**).

the frontal cortex. These cells were identified as microglial cells as they co-expressed nestin and the CD11b marker (Figure 3F). In contrast, nestin$^+$ microglial cells could not be detected in the frontal cortex of P15 KΔ75 (Figure 3G) whereas nestin$^+$ neural stem cells located in the frontal subventricular zone were clearly present in both P15 KΔ75 and WT mice (Figure 3; I to L).

Increased Bone Mass in KΔ75 Mice

Because PLOSL patients suffer from both brain and bone damage, we then investigated bone phenotype in KΔ75 mice. Whole-body X-ray analysis was performed on 5-month-old WT and KΔ75 mice and, in contrast to human patients, no bone cysts could be observed. Contrary to the human pathology, radiographs of femurs isolated from KΔ75 mutant mice showed a significant increase in trabecular bone density as compared to femurs isolated from control mice (Figure 5A, rectangles), as well as thickening of the cortical bone (Figure 5A, arrows). Indeed, transversal sections of femurs clearly showed a 25% increase in cortical bone thickness in mutant mice as compared to WT controls (Figure 5B). This effect of the KARAP/DAP12 mutation on bone phenotype was further confirmed by DEXA analysis, which showed that in KΔ75 mice, bone mineral content as well as bone mineral density were significantly increased (Figure 5C). Histomorphometric analysis also showed a doubling of trabecular bone volume (BV/TV) in mutant mice, reflected in an increase in trabecular numbers (Tb N) and a decrease in trabecular separation (Tb Sp) (Figure 5D).

Reduced Bone Remodeling in KΔ75 Mice

Taking into account bone remodeling, the bone mass increase observed in KΔ75 mice could be because of an increased osteoblast-mediated formation, or reduced osteoclast-mediated degradation or both. Urinary levels of deoxypyridinoline (U-DPD), a collagen degradation byproduct that is a marker of bone matrix degradation, were significantly reduced in KΔ75 mice as compared to WT mice (Figure 6A) indicating that osteoclast-mediated bone resorption was impaired. Surprisingly, observation of bone slices stained to show osteoclast TRAP activity did not support a reduction in osteoclast numbers (Figure 6B). In contrast, double labeling with calcein indicated that in KARAP/DAP12 KI mice, bone formation rate (BFR) was reduced by more than 50% when compared to WT (Figure 6C). This was concomitant to a similar reduction in mineralizing surfaces (MS/BS; Figure 6D), whereas mineral apposition rate, which reflects osteoblast activity, was the same in WT and KI mice (Figure 6E). Altogether, these results suggest that bone remodeling was strongly reduced in KΔ75 mice, because of a defect in bone resorption. Thus, ITAM-deficient KARAP molecules led to *in vivo* osteoclast function alterations leading to mild but significant osteopetrosis consistent with the phenotype observed in the complete absence of the gene[16–19] but different from human PLOSL.

Impaired in Vitro *Osteoclast Differentiation and* in Vivo *Osteoclast Function in KΔ75 Mice*

Since it has been reported that KARAP/DAP12 inactivation in mice as well as TREM-2 mutations in humans alter osteoclast differentiation,[13–19] we investigated whether this was also true with KΔ75 mice. To this aim, bone marrow cells isolated from 6- to 8-week-old WT and KΔ75 mice were cultured *in vitro*, in the presence of 1,25(OH)$_2$ vitamin D3 (VD3; 10^{-8} mol/L) or parathyroid hormone (PTH; 10^{-7} mol/L), two osteotropic agents known to promote osteoclast differentiation through osteoblast stimulation.[34] Whereas numerous large TRAP$^+$ multinucleated osteoclasts could be obtained from WT mice, only a few small osteoclasts were obtained from KΔ75 mice with either VD3 or PTH, suggesting an osteoclast defect (Figure 7, A and B). To confirm this result, bone marrow cells

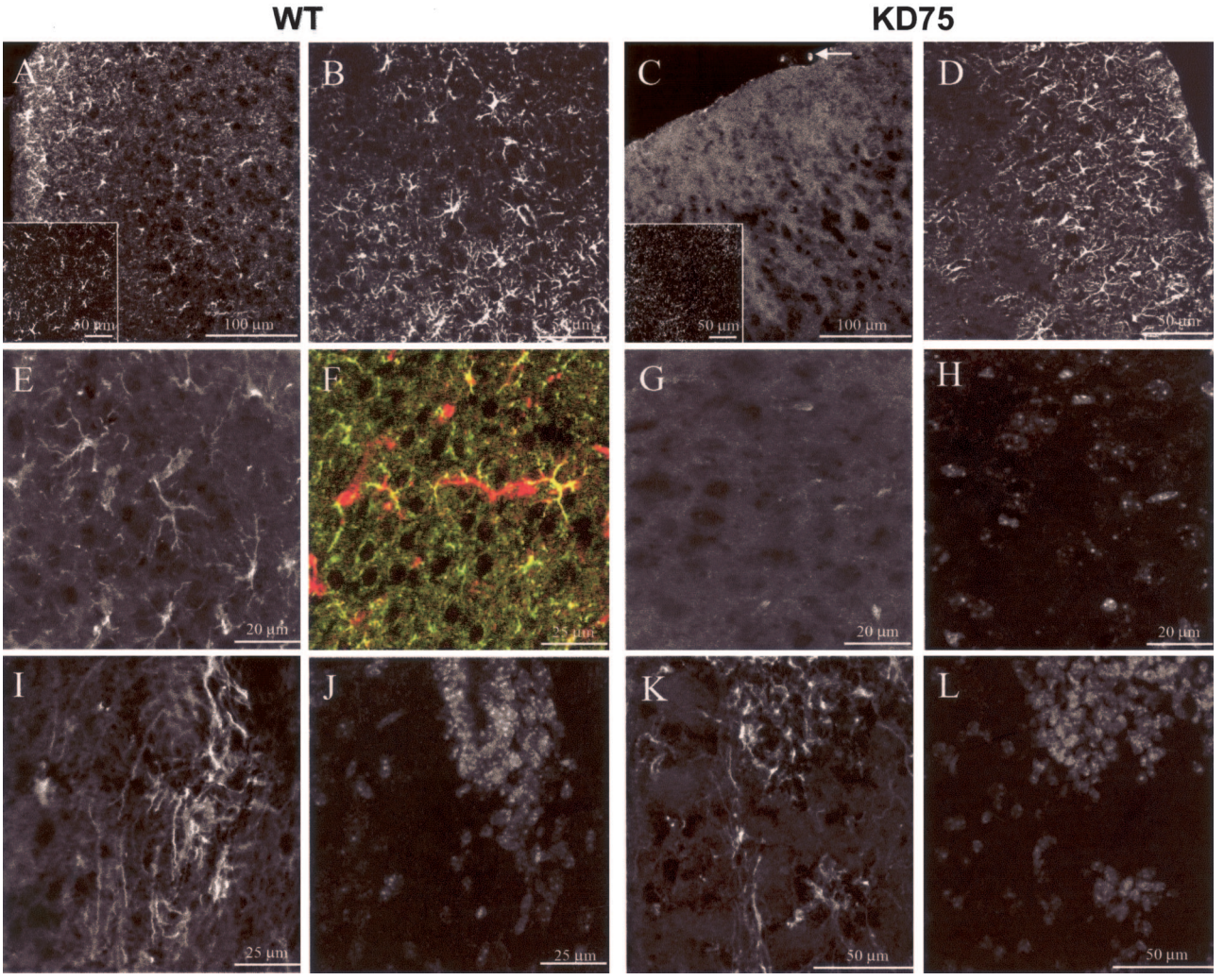

Figure 3. Immunohistofluorescence analysis of postnatal microglia in KΔ75 mice. **A–L:** Immunohistofluorescence experiments were performed on transverse sections of anterior brain obtained from control postnatal 15-day WT (**left**; **A**, **B**, **E**, **F**, **I**, **J**) or KΔ75 mice (**right**; **C**, **D**, **G**, **H**, **K**, **L**). CD11b staining (**A**, **C**) shows that as opposed to controls (**A**), KΔ75 mice lack detectable microglial cells (**C**). However meningeal macrophages are still present in KΔ75 mice (**white arrow** in **C**). **Insets** in **A** and **C** show confocal images of CD11b staining in control (**A**) or KΔ75 mice (**C**). Note that only background fluorescence and no cellular CD11b staining is observable by confocal analysis in KΔ75 mice (**inset** in **C**). GFAP staining (**B** and **D**) is unaltered in KΔ75 as compared to WT mice. Nestin staining of frontal cortex sections (**E–G**) allows ramified cells to be detected (**E**, white; **F**, red) co-expressing CD11b (**F**, green) in WT (**E**, **F**) but not in KΔ75 mice (**G**, counterstained with DAPI in **H**). Nestin$^+$ cells are detectable in the frontal subventricular zone of WT (**I**, counterstained with DAPI in **J**) or KΔ75 mice (**K**, counterstained with DAPI in **L**). Data are representative of three experiments performed on six mice analyzed on P15 and five mice analyzed on P10 (CD11b staining only for P10 brains).

from both types of mice were grown in the presence of M-CSF plus RANKL, the two osteoclastogenic growth factors. No TRAP$^+$ osteoclasts were detected in bone marrow cell cultures prepared from KΔ75 mice, in marked contrast to control cultures (Figure 7B). Moreover, when cultured on dentin slices, numerous resorption pits were observed in the presence of differentiated WT osteoclasts, while dentin slices were intact in cultures of bone marrow cells isolated from KΔ75 mice (Figure 7C). Taken together, these results confirmed that *in vitro*, KARAP/DAP12-mediated signals are required for inducing osteoclast differentiation from bone marrow precursors.

The presence of osteoclasts in mutant KΔ75 mice and their mild osteopetrotic phenotype fits in with a reduced osteoclast activity *in vivo*, but does not fit well with the almost complete blocking of osteoclast differentiation observed *in vitro*. To gain further insight into osteoclast differentiation *in vitro* and *in vivo* we compared the expression levels of two osteoclast genes, namely cathepsin K and calcitonin receptor (CTR) in bones from 10-week-old WT and KΔ75 mice as well as in bone marrow cultures maintained in the presence of M-CSF plus RANKL. Our results confirmed the almost complete blocking of the osteoclast differentiation pathway *in vitro* because CTR and cathepsin K mRNA were barely detectable in cultures from KΔ75 mice (Figure 7D, left). Strikingly, bones from WT and KΔ75 mice expressed identical levels of the two markers (Figure 7D, right). These results confirmed that, in KΔ75 mice, as in KARAP/DAP12-deficient mice, osteoclast differentiation can take place but osteoclast resorption ability is altered, leading to osteopetrosis, in contrast to *in vitro* in which osteoclast differentiation is

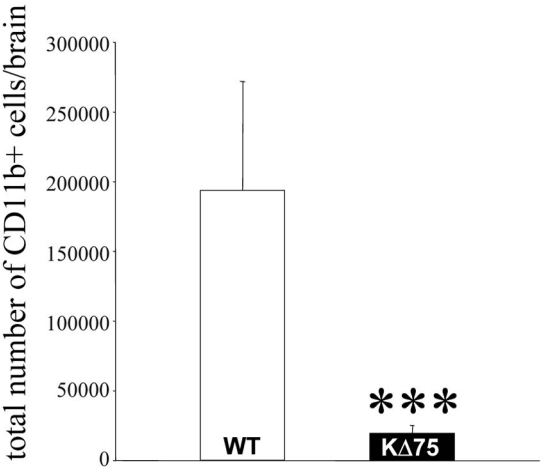

Figure 4. FACS analysis of postnatal microglia in KΔ75 mice. Total $CD11b^+$ cell number per brain was evaluated by *ex vivo* FACS analysis of brain obtained from P13 WT ($n = 6$) or KΔ75 mice. ***, $P < 0.01$ with unequal variance, Student's *t*-test.

completely impaired. Our results, together with the results published by Mocsai and colleagues[18] and Koga and colleagues[17] emphasize the importance of the ITAM-signaling pathway dependent on ITAM-bearing polypeptides in osteoclast differentiation.

Selective Block of Microglia and Osteoclast Differentiation from Common Monocytic Precursors

Previously published results, as well as those presented here, suggest that KARAP/DAP12 mediates specific signals controlling both microglia[16] and osteoclast pathways.[16–19] Nevertheless, functional DCs can be obtained from KΔ75 mice. We then decided to investigate the involvement of KARAP/DAP12 in monocytic progenitor commitment. We have previously shown that in mice, the FLT3-Ligand (FL) amplifies a population of bone marrow-derived monocytic precursors with the ability to differentiate into macrophages, osteoclasts, DCs, or microglial cells when grown in the presence of M-CSF, M-CSF plus RANKL, GM-CSF plus tumor necrosis factor-α, or glia-cell conditioned medium, respectively.[23] We made use of this *in vitro* model to further dissect the role of KARAP/DAP12 in the monocytic precursor commitment. Bone marrow cells from WT or KΔ75 mice were first amplified in the presence of FL (5 ng/ml) and then switched to specific conditioned media. In the presence of M-CSF, functional

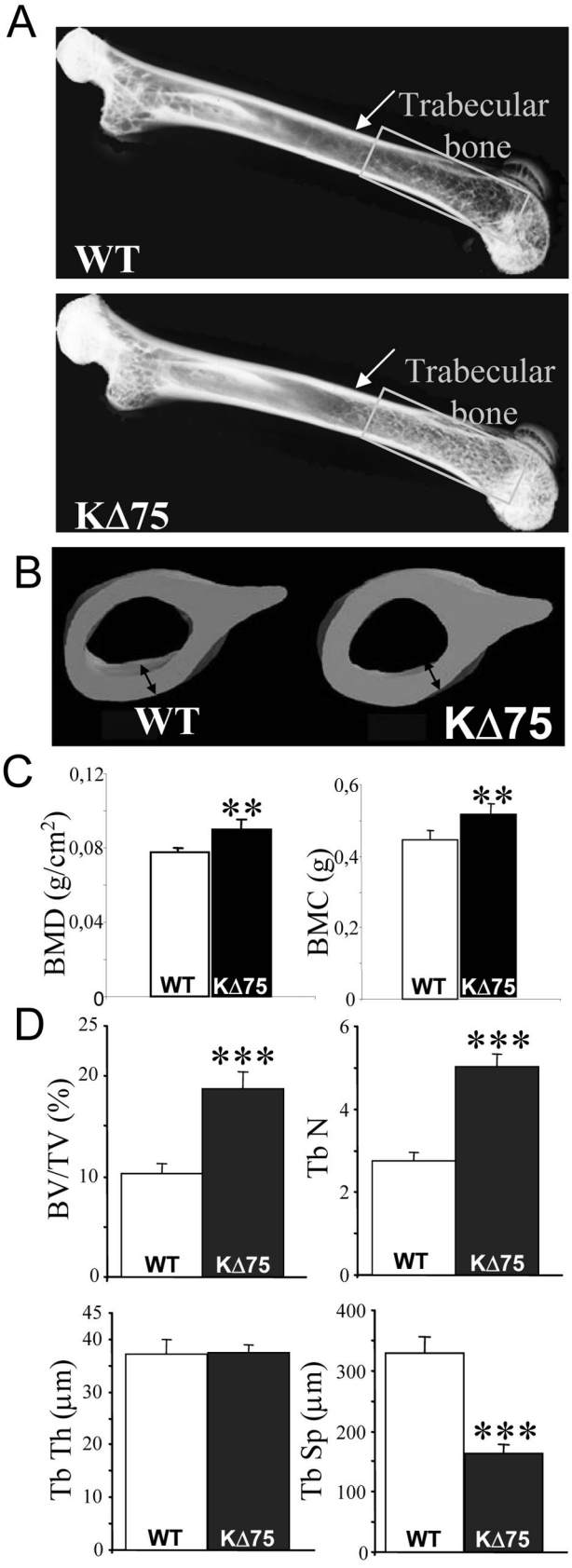

Figure 5. *In vivo* analysis of bone remodeling in KΔ75 loss-of-function mice. **A:** X-ray radiographs of femurs isolated from control C57BL/6 (**top**) and 5-month-old KΔ75 mice (**bottom**). Cortical bone in the metaphysis is indicated by an **arrow** whereas the trabecular bone area in the epiphysis is underlined by **rectangles**. Images are representative of six mice analyzed for each genotype. **B:** Micro-CT three-dimensional analysis of femurs isolated from the same WT (**left**) and KΔ75 (**right**) mice as in **A**. **Double-headed arrows** point to cortical bone thickness. **C:** DEXA quantification of bone mineral content (BMC) and evaluation of bone mineral density (BMD) of 5-month-old control and KΔ75 mice ($n = 7$). **D:** Histomorphometric measures on tibiae of 5-month-old control and KΔ75 mice: bone volume/tissue volume (BV/TV), trabecular number (Tb N), trabecular thickness (Tb Th), and trabecular separation (Tb Sp) are indicated ($n = 7$).

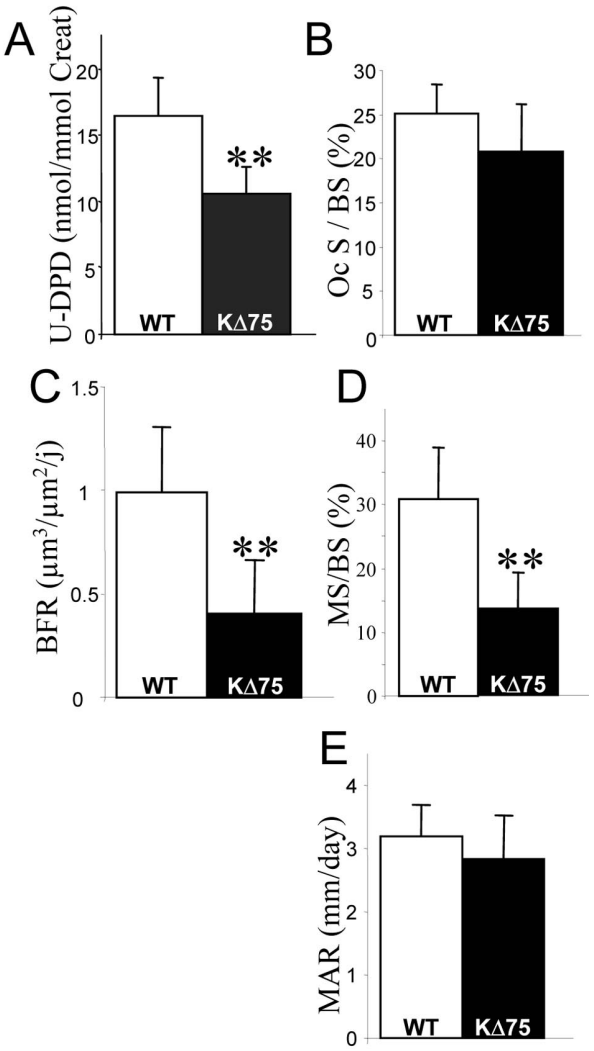

Figure 6. Physiological analysis of bone remodeling by histomorphometry. **A:** Urinary DPD levels analyzed in control (**open bars**) and KΔ75 mice (**filled bars**) are expressed as mean ± SEM and were performed on the same two groups of six mice. Histomorphometric dynamic parameters: percentage of bone trabecular surface covered by $TRAP^+$ osteoclasts (Oc S/BS) (**B**); bone formation rate (BFR) (**C**); percentage of bone trabecular surface labeled with calcein (MS/BS) (**D**); mineral apposition rate (MAR) (**E**). All results have been analyzed by the Student's *t*-test (**, $P < 0.01$) with measurements on at least six animals.

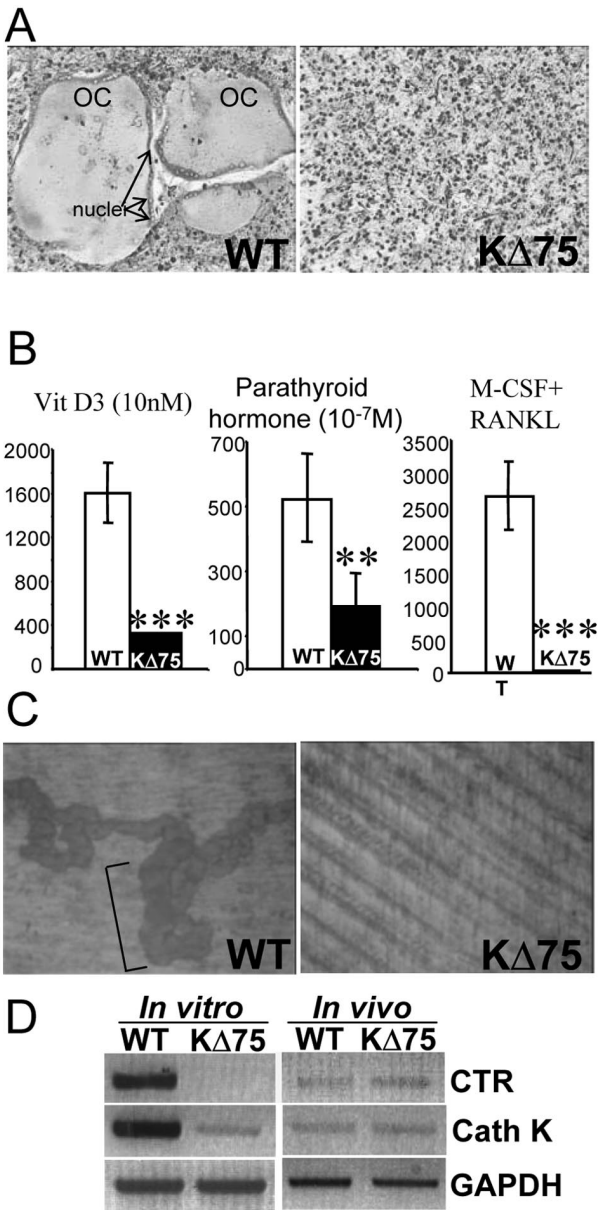

Figure 7. *In vitro* differentiation of osteoclasts in the absence of KARAP/DAP12-mediated signaling. **A:** Osteoclasts were differentiated *in vitro* from control (**left**) and KΔ75 mice (**right**) bone marrow cells in the presence of M-CSF plus RANKL and then stained for TRAP activity. Large multinucleated TRAP-positive cells (OC) were obtained from WT but none from KΔ75 mice bone marrows. **Arrows** point to nuclei of multinucleated TRAP-positive osteoclasts. **B:** Osteoclast differentiation yields obtained using indicated stimuli from cultures of control (**open bars**) and KΔ75 (**filled bars**) bone marrow cells are represented by mean ± SEM of number of $TRAP^+$ cells. Results from three independent experiments have been analyzed by the Student's *t*-test (***, $P < 0.001$; **, $P < 0.01$). **C:** Osteoclasts were differentiated *in vitro*, in the presence of M-CSF plus RANKL, directly onto dentin slices. On day 7 of culture, resorption activity was evaluated in culture of control (**left**) and KΔ75 (**right**) bone marrow cells. Typical pits (**brackets**) are observed with WT but none with KΔ75-derived bone marrow cells. **D:** KΔ75 mice-derived osteoclast differentiation pathway is blocked early *in vitro* whereas osteoclast function is altered *in vivo*. Cathepsin K (Cath K) and calcitonin receptor (CTR) expression levels from either osteoclasts obtained *in vitro* from bone marrow cells maintained for a week in the presence of M-CSF and RANKL or directly from bones, were assessed by reverse transcriptase-polymerase chain reaction. Osteoclasts obtained *in vitro* from KΔ75 mice expressed almost undetectable levels of cathepsin K and CTR in comparison with WT-derived osteoclasts (**left**). In contrast, both genes were expressed at the same levels in both KΔ75- and WT-derived bones (**right**). GAPDH mRNA level was used as an internal control. The results presented here are representative of at least three different experiments.

macrophages, able to phagocytize latex beads (Figure 8A), as well as DCs, in presence of GM-CSF plus tumor necrosis factor-α (Figure 8B) were obtained from both types of mice. In sharp contrast, neither multinucleated osteoclasts (Figure 8C) nor microglial cells (Figure 8D) could be obtained from KΔ75 mice FL-amplified monocytic progenitors confirming a selective block in the differentiation pathway of these two monocytic-derived cells. This suggests that, in this experimental model, KARAP/DAP12-dependant signaling could play a specific role along these two monocyte-derived lineages.

Discussion

We have investigated whether in mice, as previously described in PLOSL patients, the absence of KARAP/

DAP12-mediated signals through its ITAM domain, can affect brain and bone homeostasis.[10,11] To this aim, we have examined the CNS and skeleton of KΔ75 mice, harboring a truncated KARAP/DAP12 ITAM motif.[25]

The main neuropathological finding observed in adult KΔ75 mice is a hypomyelination that predominates in myelin-rich anterior brain regions. Although such an observation is in accordance with the reported presence of myelin defects in the anterior brain of PLOSL patients, a number of pathological features that characterize PLOSL are not present in KΔ75 mice. These include microglial activation, myelin phagocytosis by activated microglia/macrophages, astrocytosis, axonal and neuronal cell loss, basal ganglial calcification, and thickening of the microvessel wall. The fact that defective myelination rather than demyelination occurs in KΔ75 mice, suggests that myelin formation and/or turnover is altered in KΔ75 mice. This is in accordance with previous work showing abnormal oligodendrocyte development in KARAP/DAP12 knockout mice.[16] However, the mechanisms leading to an altered myelin formation in the absence of KARAP/DAP12-mediated signals have not yet been elucidated. Although Kaifu and colleagues[16] reported KARAP/DAP12 expression *in vitro* on myelinating oligodendrocytes, the precise *in vivo* distribution of KARAP/DAP12 within human or rodent brain remains uncertain. The same observation applies to TREM-2, although its expression has been described in microglia.[35] Interestingly, the expression and function of another ITAM-bearing adaptor protein, FcRγ, was recently demonstrated in the oligodendrocyte lineage.[36] Therefore, one can postulate that DAP-12 in oligodendrocytes is a major signaling molecule involved in the transducing pathway of several ITAM receptors including TREM and FcRγ. Alternatively and despite DAP-12 expression by oligodendrocytes, one might hypothesize that the KARAP/DAP12 deficiency primarily affects microglia and that hypomyelination is indeed a consequence of abnormal microglial cell function. Supporting this view, we found that KΔ75 mice present major *in vitro* and *in vivo* alterations of microglial cell development. This is of interest because activated neonatal microglia are known to secrete a number of neurotrophic factors, such as nerve growth factor and neurotrophin-3, which may stimulate oligodendrocyte maturation.[37,38] Also, we describe for the first time a microglial cell subpopulation expressing the neural stem cell marker nestin in developing brain. This population was absent from KΔ75 mice when nestin$^+$ periventricular neural stem cells were still detectable. Interestingly, nestin$^+$ microglial cells were recently shown to behave *in vitro* as neural stem cells and to generate neurons, astrocytes, or oligodendrocytes.[32] In the same way, cells co-expressing oligodendrocyte and

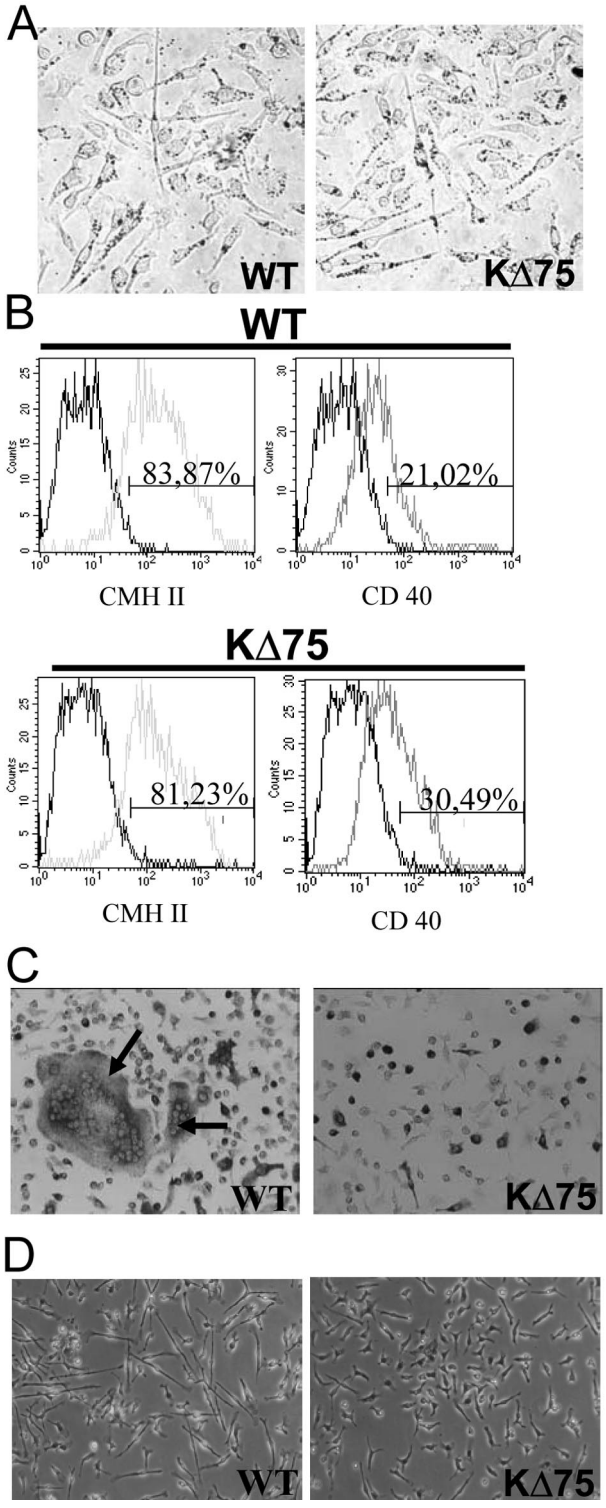

Figure 8. Differentiation of Flt3L-amplified cells in monocytic lineages. Bone marrow cells from control or KΔ75 mice were amplified *in vitro* in Flt3L for 6 to 11 days and differentiated as indicated below. **A:** For macrophage differentiation, Flt3L-amplified cells were cultured in the presence of M-CSF for 5 days and their ability to phagocyte latex beads was evaluated (**dots** in the cytoplasm). **B:** For DC differentiation, Flt3L-amplified cells were cultured in the presence of GM-CSF plus tumor necrosis factor-α for 6 days. The expression of the MHC II and CD40 antigen was evaluated by flow cytometry. **C:** For osteoclast differentiation, Flt3L-amplified cells were cultured in the presence of M-CSF plus RANKL for 6 days. The presence of osteoclasts was evaluated by TRAP staining and cell morphology (number of nuclei). **Arrows** point to osteoclasts. **D:** For microglial cell differentiation, bone marrow cells, amplified with Flt3L for 11 days, were cultured in the presence of GCCM. After 4 days of culture, ramified cells, defined as cells displaying at least one process three times longer than the cell body diameter, were very sparse in cultures derived from KΔ75 mice whereas they represented more than 20% of cells in cultures derived from WT mice. The results presented here are representative of at least three different experiments.

microglial cell markers were detected in the human developing brain.[39] Altogether, these results, together with ours, raise the intriguing possibility that besides the conventional pathway of oligodendrocyte development from neural stem cells, a subset of oligodendrocytes may actually derive from KARAP/DAP12-expressing microglial cells.[32] If so, defective activation of microglia KARAP/DAP12 signaling may alter microglial cell differentiation toward oligodendrocyte and ultimately lead to hypomyelination. Moreover, the reported expression of KARAP/DAP12 in oligodendrocytes[16] may indeed reflect a lineage relationship between microglia and oligodendrocytes.

Our results also provide a complete bone histomorphological analysis of KΔ75 mice, as compared to WT mice, indicating that bone mineral density, as well as bone mineral content, are significantly increased. Cortical bone is increased by ~25% and trabeculae in the metaphysis of long bones are more abundant, with an equivalent thickness. We have shown that bone matrix deposition and mineralization by individual osteoblasts are normal, but overall bone formation is lower when balanced against decreased bone resorption, resulting in a reduced remodeling with mild osteopetrosis consistent with previous results obtained with KARAP/DAP12-null mice.[16–19] Similarly, osteoclast precursors from KΔ75-deficient mice grown *in vitro* in the presence of M-CSF and RANKL are unable to form multinucleated osteoclasts. Thus, in mutant mice, osteoclasts are present but harbor altered bone resorption properties and cannot differentiate from myeloid progenitors *in vitro*. This discrepancy between *in vitro* and *in vivo* data can be explained by the existence of newly discovered osteoclast differentiation and signaling pathways. Indeed, it has been shown very recently that RANKL and M-CSF are not sufficient to activate the signals required for osteoclastogenesis.[17,18] In addition, complete osteoclastogenesis requires another signaling pathway through KARAP/DAP12 and FcRγ adaptors linked to receptors such as TREM-2 and OSCAR, respectively. Ligands for these receptors are still unknown but must be provided by cells of the bone microenvironment.[17,40]

We also provide preliminary evidence that the ITAM-signaling pathway could play a selective role in the differentiation of various cell types derived from a common monocytic origin. Within the limits of our model of FLT3-ligand-amplified monocytic progenitors, we suggest that macrophage and DC pathways are not controlled by KARAP/DAP12 whereas KARAP/DAP12 is mandatory for osteoclast and microglial cell commitment *in vitro*. It is possible that the involvement of this ITAM-harboring adaptor is different in both cell lineages because in KΔ75 mice, osteoclasts are present *in vivo* but with altered functions whereas the microglial cell number is decreased *in vivo*, suggesting different levels of activity. Whether the same co-receptors are involved in osteoclast and microglial precursors is still unknown.

The data presented here and by others[16–19] clearly show that in both KΔ75 mutant mice and in human PLOSL patients, the CNS and bone are affected. However, these results show that the pathological features observed in both species are far from being equivalent. Indeed, clinical and histomorphological alterations of the CNS are much less dramatic in mice than in humans, and KΔ75 mice do not show any obvious behavioral abnormalities (D. Montag, personal communication). At bone level, KΔ75 as well as KARAP/DAP12-deficient mice do not display spontaneous fractures or bone cysts but do display mild osteopetrosis. It still remains to be determined whether the massive brain inflammation and blood vessel damage observed in PLOSL patients are secondary to defective myelinogenesis or directly related to KARAP/DAP12 deficiency. The absence of microglial and astrocyte activation in mice deficient for KARAP/DAP12 does not support this latter hypothesis. Several other epigenetic factors could correlate KARAP/DAP12 deficiency with the complex bone and CNS pathology observed in humans and mice. In this context, the PLOSL pathology has been reported in restricted geographic and ethnic areas, suggesting that the severity of this disease could be the result of a KARAP/DAP12 deficiency associated with a selective genetic background. Along these lines, susceptibility factors under the influence of epistatic modifiers have been identified for the development of autoimmunity in the case of FcγRIIB.[41] It is also possible that environmental factors could represent a link between inadequate immune response, related to KARAP/DAP12 deficiency, and bone as well as brain symptoms. In contrast to what has been reported for mice,[25] no increased sensitivity to microbial infections or frequency of malignancies has been detected in human PLOSL patients. Nevertheless, it still remains to be determined whether, in the absence of KARAP/DAP12-mediated signals, human immune responses could not be modified in such a way that they could contribute to the onset and/or the progression of the PLOSL disorder.

Acknowledgments

We thank Pr. J. Tanaka (Ehime University, Japan) for critical reading of the manuscript, Dr. P. Clezardin (INSERM U403, Lyon) for use of his X-ray equipment, Dr. Takahashi (Nagano, Japan) for the generous gift of dentin slices, François Duboeuf and Jean-Paul Roux (U403) for their technical assistance, and Simone Peyrol and Christel Cassin (CECIL, Laennec Faculty, Lyon) for EM studies, and the Consortium National du Reseau des Genopoles for funding the ANIMAGE platform.

References

1. Olcese L, Cambiaggi A, Semenzato G, Bottino C, Moretta A, Vivier E: Human killer cell activatory receptors for MHC class I molecules are included in a multimeric complex expressed by natural killer cells. J Immunol 1997, 158:5083–5086
2. Lanier LL, Corliss BC, Wu J, Leong C, Phillips JH: Immunoreceptor DAP12 bearing a tyrosine-based activation motif is involved in activating NK cells. Nature 1998, 391:703–707
3. Tomasello E, Blery M, Vely F, Vivier E: Signaling pathways engaged by NK cell receptors: double concerto for activating receptors, inhibitory receptors and NK cells. Semin Immunol 2000, 12:139–147
4. Moretta A, Bottino C, Vitale M, Pende D, Cantoni C, Mingari MC, Biassoni R, Moretta L: Activating receptors and coreceptors involved

in human natural killer cell-mediated cytolysis. Annu Rev Immunol 2001, 19:197–223
5. Diefenbach A, Tomasello E, Lucas M, Jamieson AM, Hsia JK, Vivier E, Raulet DH: Selective associations with signaling proteins determine stimulatory versus costimulatory activity of NKG2D. Nat Immunol 2002, 3:1142–1149
6. Tomasello E, Cant C, Buhring HJ, Vely F, Andre P, Seiffert M, Ullrich A, Vivier E: Association of signal-regulatory proteins beta with KARAP/DAP-12. Eur J Immunol 2000, 30:2147–2156
7. Dietrich J, Cella M, Seiffert M, Buhring HJ, Colonna M: Cutting edge: signal-regulatory protein beta 1 is a DAP12-associated activating receptor expressed in myeloid cells. J Immunol 2000, 164:9–12
8. Bakker AB, Baker E, Sutherland GR, Phillips JH, Lanier LL: Myeloid DAP12-associating lectin (MDL)-1 is a cell surface receptor involved in the activation of myeloid cells. Proc Natl Acad Sci USA 1999, 96:9792–9796
9. Colonna M: TREMs in the immune system and beyond. Nat Rev Immunol 2003, 3:445–453
10. Paloneva J, Kestila M, Wu J, Salminen A, Bohling T, Ruotsalainen V, Hakola P, Bakker AB, Phillips JH, Pekkarinen P, Lanier LL, Timonen T, Peltonen L: Loss-of-function mutations in TYROBP (DAP12) result in a presenile dementia with bone cysts. Nat Genet 2000, 25:357–361
11. Paloneva J, Autti T, Raininko R, Partanen J, Salonen O, Puranen M, Hakola P, Haltia M: CNS manifestations of Nasu-Hakola disease: a frontal dementia with bone cysts. Neurology 2001, 56:1552–1558
12. Paloneva J, Manninen T, Christman G, Hovanes K, Mandelin J, Adolfsson R, Bianchin M, Bird T, Miranda R, Salmaggi A, Tranebjaerg L, Konttinen Y, Peltonen L: Mutations in two genes encoding different subunits of a receptor signaling complex result in an identical disease phenotype. Am J Hum Genet 2002, 71:656–662
13. Paloneva J, Mandelin J, Kiialainen A, Bohling T, Prudlo J, Hakola P, Haltia M, Konttinen YT, Peltonen L: DAP12/TREM2 deficiency results in impaired osteoclast differentiation and osteoporotic features. J Exp Med 2003, 198:669–675
14. Cella M, Buonsanti C, Strader C, Kondo T, Salmaggi A, Colonna M: Impaired differentiation of osteoclasts in TREM-2-deficient individuals. J Exp Med 2003, 198:645–651
15. Humphrey MB, Ogasawara K, Yao W, Spusta SC, Daws MR, Lane NE, Lanier LL, Nakamura MC: The signaling adapter protein DAP12 regulates multinucleation during osteoclast development. J Bone Miner Res 2004, 19:224–234
16. Kaifu T, Nakahara J, Inui M, Mishima K, Momiyama T, Kaji M, Sugahara A, Koito H, Ujike-Asai A, Nakamura A, Kanazawa K, Tan-Takeuchi K, Iwasaki K, Yokoyama WM, Kudo A, Fujiwara M, Asou H, Takai T: Osteopetrosis and thalamic hypomyelinosis with synaptic degeneration in DAP12-deficient mice. J Clin Invest 2003, 111:323–332
17. Koga T, Inui M, Inoue K, Kim S, Suematsu A, Kobayashi E, Iwata T, Ohnishi H, Matozaki T, Kodama T, Taniguchi T, Takayanagi H, Takai T: Costimulatory signals mediated by the ITAM motif cooperate with RANKL for bone homeostasis. Nature 2004, 428:758–763
18. Mocsai A, Humphrey MB, Van Ziffle JA, Hu Y, Burghardt A, Spusta SC, Majumdar S, Lanier LL, Lowell CA, Nakamura MC: The immunomodulatory adapter proteins DAP12 and Fc receptor gamma-chain (FcRgamma) regulate development of functional osteoclasts through the Syk tyrosine kinase. Proc Natl Acad Sci USA 2004, 101:6158–6163
19. Faccio R, Zou W, Colaianni G, Teitelbaum SL, Ross FP: High dose M-CSF partially rescues the Dap12−/− osteoclast phenotype. J Cell Biochem 2003, 90:871–883
20. Charles P, Hernandez MP, Stankoff B, Aigrot MS, Colin C, Rougon G, Zalc B, Lubetzki C: Negative regulation of central nervous system myelination by polysialylated-neural cell adhesion molecule. Proc Natl Acad Sci USA 2000, 97:7585–7590
21. John GR, Shankar SL, Shafit-Zagardo B, Massimi A, Lee SC, Raine CS, Brosnan CF: Multiple sclerosis: re-expression of a developmental pathway that restricts oligodendrocyte maturation. Nat Med 2002, 8:1115–1121
22. Vitry S, Bertrand JY, Cumano A, Dubois-Dalcq M: Primordial hematopoietic stem cells generate microglia but not myelin-forming cells in a neural environment. J Neurosci 2003, 23:10724–10731
23. Servet-Delprat C, Arnaud S, Jurdic P, Nataf S, Grasset MF, Soulas C, Domenget C, Destaing O, Rivollier A, Perret M, Dumontel C, Hanau D, Gilmore GL, Belin MF, Rabourdin-Combe C, Mouchiroud G: Flt3+ macrophage precursors commit sequentially to osteoclasts, dendritic cells and microglia. BMC Immunol 2002, 3:15–25
24. Boyle WJ, Simonet WS, Lacey DL: Osteoclast differentiation and activation. Nature 2003, 423:337–342
25. Tomasello E, Desmoulins PO, Chemin K, Guia S, Cremer H, Ortaldo J, Love P, Kaiserlian D, Vivier E: Combined natural killer cell and dendritic cell functional deficiency in KARAP/DAP12 loss-of-function mutant mice. Immunity 2000, 13:355–364
26. Giulian D, Li J, Bartel S, Broker J, Li X, Kirkpatrick JB: Cell surface morphology identifies microglia as a distinct class of mononuclear phagocyte. J Neurosci 1995, 15:7712–7726
27. Solari F, Flamant F, Cherel Y, Wyers M, Jurdic P: The osteoclast generation: an in vitro and in vivo study with a genetically labelled avian monocytic cell line. J Cell Sci 1996, 109:1203–1213
28. Camelo S, Lafage M, Lafon M: Absence of the p55 Kd TNF-alpha receptor promotes survival in rabies virus acute encephalitis. J Neurovirol 2000, 6:507–518
29. Parfitt AM, Drezner MK, Glorieux FH, Kanis JA, Malluche H, Meunier PJ, Ott SM, Recker RR: Bone histomorphometry: standardization of nomenclature, symbols, and units. Report of the ASBMR Histomorphometry Nomenclature Committee. J Bone Miner Res 1987, 2:595–610
30. Alliot F, Godin I, Pessac B: Microglia derive from progenitors, originating from the yolk sac, and which proliferate in the brain. Brain Res Dev Brain Res 1999, 117:145–152
31. Ling EA, Wong WC: The origin and nature of ramified and amoeboid microglia: a historical review and current concepts. Glia 1993, 7:9–18
32. Yokoyama A, Yang L, Itoh S, Mori K, Tanaka J: Microglia, a potential source of neurons, astrocytes, and oligodendrocytes. Glia 2004, 45:96–104
33. Sahin Kaya S, Mahmood A, Li Y, Yavuz E, Chopp M: Expression of nestin after traumatic brain injury in rat brain. Brain Res 1999, 840:153–157
34. Horwood NJ, Elliott J, Martin TJ, Gillespie MT: Osteotropic agents regulate the expression of osteoclast differentiation factor and osteoprotegerin in osteoblastic stromal cells. Endocrinology 1998, 139:4743–4746
35. Schmid CD, Sautkulis LN, Danielson PE, Cooper J, Hasel KW, Hilbush BS, Sutcliffe JG, Carson MJ: Heterogeneous expression of the triggering receptor expressed on myeloid cells-2 on adult murine microglia. J Neurochem 2002, 83:1309–1320
36. Nakahara J, Tan-Takeuchi K, Seiwa C, Gotoh M, Kaifu T, Ujike A, Inui M, Yagi T, Ogawa M, Aiso S, Takai T, Asou H: Signaling via immunoglobulin Fc receptors induces oligodendrocyte precursor cell differentiation. Dev Cell 2003, 4:841–852
37. Elkabes S, DiCicco-Bloom EM, Black IB: Brain microglia/macrophages express neurotrophins that selectively regulate microglial proliferation and function. J Neurosci 1996, 16:2508–2521
38. Yan H, Wood PM: NT-3 weakly stimulates proliferation of adult rat O1(−)O4(+) oligodendrocyte-lineage cells and increases oligodendrocyte myelination in vitro. J Neurosci Res 2000, 62:329–335
39. Rakic S, Zecevic N: Early oligodendrocyte progenitor cells in the human fetal telencephalon. Glia 2003, 41:117–127
40. Baron R: Arming the osteoclast. Nat Med 2004, 10:458–460
41. Bolland S, Ravetch JV: Spontaneous autoimmune disease in Fc(gamma)RIIB-deficient mice results from strain-specific epistasis. Immunity 2000, 13:277–285